

**APPENDIX G**

**SUMMARY OF RECENT INFORMATION RELEVANT TO THE  
SATURATED ZONE PROCESS MODEL**

INTENTIONALLY LEFT BLANK

## **SUMMARY OF RECENT INFORMATION RELEVANT TO THE SATURATED ZONE PROCESS MODEL**

### **1. INTRODUCTION**

This white paper contains a summary of recent test results and other additional information that are relevant to the saturated zone (SZ) process model used to support the *Yucca Mountain Science and Engineering Report* (YMS&ER) (DOE 2001a) and the *Yucca Mountain Preliminary Site Suitability Evaluation* (YMPSSSE) (DOE 2001b). The U.S. Department of Energy (DOE) released these two documents for public review in May and August, respectively, of this year.

The white paper focuses on the results of those field and laboratory tests and other additional information that became available after the SZ process model was completed to support the preparation of the YMS&ER and the YMPSSSE. The summary of this recent information is being used to conduct an impact review in accordance with AP-2.14Q, *Review of Technical Products and Data*, to determine if this additional information has any impact on the technical analyses supporting the YMS&ER and the YMPSSSE. The documentation of the additional information in this white paper is an interim step and primarily used to support this impact review. This information is expected to be formally documented in subsequent Project technical reports, as appropriate.

To assist in the impact review, this white paper briefly describes the SZ process model that was used to support the YMS&ER and the YMPSSSE, provides a summary of the recent test results and other additional information, and discusses the potential implications of this more recent information on our understanding of the SZ process model.

### **2. SUMMARY DESCRIPTION OF THE SATURATED ZONE PROCESS MODEL**

This section provides a brief description of the process model that was used to support the YMS&ER (DOE 2001a) and the YMPSSSE (DOE 2001b). The SZ system is expected to act as a barrier to the movement of radionuclides by delaying the transport of radionuclides to the accessible environment and by reducing the concentration of radionuclides before they reach the accessible environment. Information obtained from Yucca Mountain Site Characterization Project activities is used to estimate groundwater flow rates through the site-scale SZ flow and transport model area and to constrain general conceptual models of groundwater flow in the site-scale area. The site-scale conceptual model is a synthesis of what is known about flow and transport processes at the scale required for the *Total System Performance Assessment for the Site Recommendation* (TSPA-SR) (CRWMS M&O 2000a) calculations and Volume 1 of *FY01 Supplemental Science for Performance Analyses* (BSC 2001a). This knowledge builds on and is consistent with knowledge that has accumulated at the regional scale but is more detailed because more data are available at the site-scale level. The mathematical basis of the site-scale model and the associated numerical approaches are designed to assist in quantifying the uncertainty in the permeability of rocks in the geologic framework model and to represent accurately the flow and transport processes included in the site-scale conceptual model. An inverse approach was used to estimate the distribution of rock permeability that resulted in calculated values of hydraulic head that best match measured values. An inverse approach also was used to calculate rates of lateral flow across model boundaries that are compatible with

results of the regional-scale flow model. Confidence in the results of the mathematical model was increased by comparing calculated to observed hydraulic heads, estimated to measured permeabilities, and lateral flow rates calculated by the site-scale model to those calculated by the regional-scale flow model. In addition, it was confirmed that the flow paths leaving the region of the potential repository are consistent with those inferred from gradients of measured head and those independently inferred from water chemistry data. The key processes incorporated in the site-scale SZ flow and transport model are abstracted for use in the TSPA. The general approach of the site-scale SZ flow and transport model analysis is to calculate unit breakthrough curves for radionuclides at the interface between the SZ and the biosphere using the three-dimensional site-scale SZ flow and transport model. Uncertainties are explicitly incorporated into the TSPA site-scale SZ flow and transport abstractions through key parameters and conceptual models.

### **3. SUMMARY OF RECENT TEST RESULTS AND OTHER ADDITIONAL INFORMATION**

This section summarizes recent results obtained from the different field and laboratory tests and other modeling and analyses that have provided information relevant to enhancing our understanding of the SZ process model. The field and laboratory tests, modeling, and analyses that provided this additional information are listed below and discussed in each of the sections that follow.

1. Stratigraphy from new Nye County Early Warning Drilling Program wells
2. Hydrochemistry data from new Nye County Early Warning Drilling Program wells
3. Hydraulic and tracer testing at the Alluvial Testing Complex
4. Calibration of different conceptual models of the large hydraulic gradient region
5. Evaluation of boundary to the accessible environment
6. Parameter sensitivity analyses
7. Uranium mill tailings sites as analogues for radionuclide transport in alluvium
8. A realistic case of saturated zone flow and transport
9. Saturated zone results from the Atomic Energy of Canada Limited (AECL) Busted Butte experiments.

Because of the recent nature of the information provided in this section, much of it is unpublished; therefore, some source references have been provided where appropriate, but others could not be provided. However, this information is currently documented in the principal investigators' scientific notebooks, if applicable, in accordance with the Project's quality assurance procedure AP-SIII.1Q, *Scientific Notebooks*.

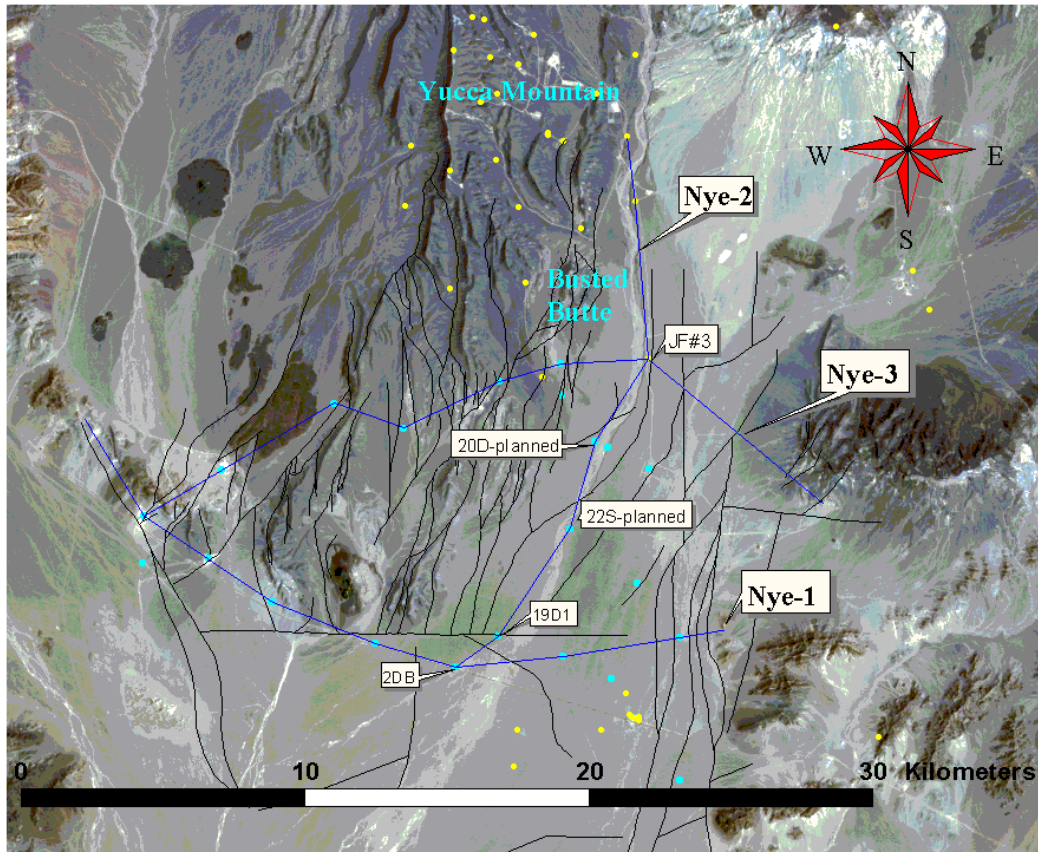
#### **3.1 STRATIGRAPHY OF THE NYE COUNTY EARLY WARNING DRILLING PROGRAM BOREHOLES**

Lithologic descriptions and stratigraphic correlation have been completed for the Phase I and Phase II boreholes, drilled under the Nye County Early Warning Drilling Program (NC-EWDP). Alluvium, pyroclastic flow and fall deposits, tuffaceous sedimentary rocks, pre-Tertiary gravel beds, and Paleozoic rocks have been identified. Unlike the central part of Yucca Mountain, the pyroclastic flow deposits that were penetrated in boreholes of Nye County's Phase I and II drilling are commonly nonwelded to partially welded and zeolitic. These pyroclastic flow

deposits are commonly intercalated with very thick sequences of siltstone and claystone of Tertiary age. North of Highway 95, these siltstone and claystone intervals give way to pyroclastic fall deposits typical of the units that separate major welded pyroclastic flow deposits within the central part of Yucca Mountain. Borehole NC-EWDP-2DB of the Phase II drilling currently represents the deepest penetration of subsurface strata, extending to a depth of 937.3 m (3,075 ft). Paleozoic quartzite, dolomite, shale, and limestone were encountered between depths of 813.8 and 937.3 m (2,670 and 3,075 ft). These lithologies are interpreted to represent rocks within the Paleozoic section. Aside from borehole UE-25 p#1, drilled north of Busted Butte, NC-EWDP-2DB represents the only other borehole that has been drilled deep enough to encounter Paleozoic rocks within the Yucca Mountain area.

Integration of recently developed subsurface geologic data, recently acquired surface-based geophysics, and surface geologic mapping has been initiated through the construction of three new geologic cross sections that extend across the Fortymile Wash and southern Yucca Mountain areas. Cross section Nye-1 is a generally east–west cross section, aligned approximately along U.S. Highway 95, near the downgradient boundary of the site-scale SZ flow and transport model. Cross section Nye-2 is a north–south cross section that generally parallels Fortymile Wash in close proximity to one of the predicted flow pathways. Cross section Nye-3, for the most part, extends across the northern part of the area of interest, in close proximity to Stage Coach Road, south of Busted Butte (Figure 1).

Information from boreholes NC-EWDP-2D, NC-EWDP-2DB of where the flow pathways from the potential repository pass from volcanic rock into alluvial deposits, and NC-EWDP-19D1 (represented in cross section Nye-2; Figure 2) is relevant to the issue because these boreholes are located along the inferred SZ flow path from Yucca Mountain. Data from boreholes NC-EWDP-2D and NC-EWDP-2DB, located between 19 and 20 km (11.8 to 12.4 mi) from the potential repository, indicate greater than 240 m (800 ft) of saturated alluvium beginning at the water table (DTN: GS000808314211.005; DTN: MO0004NC99WL2D.000). Data from borehole NC-EWDP-19D1, located approximately 19 km (11.8 mi) from the repository, show greater than 120 m (400 ft) of saturated alluvium, underlain by 130 m (440 ft) of Topopah Spring Tuff. Within NC-EWDP-19D1, the Topopah Spring Tuff is exceptionally uniform in physical properties. The unit is composed entirely of nonwelded zeolitic tuff and lacks any zonal variations that typically aid in identifying the tuff (DTN: MO0007NYE02565.024; EDCON 2000). Significant differences in the thickness and welding characteristics of the Topopah Spring Tuff occur between NC-EWDP-2DB and NC-EWDP-19D1 (approximately 1 km [0.6 mi] apart) as well as between NC-EWDP-19D1 and boreholes to the north.



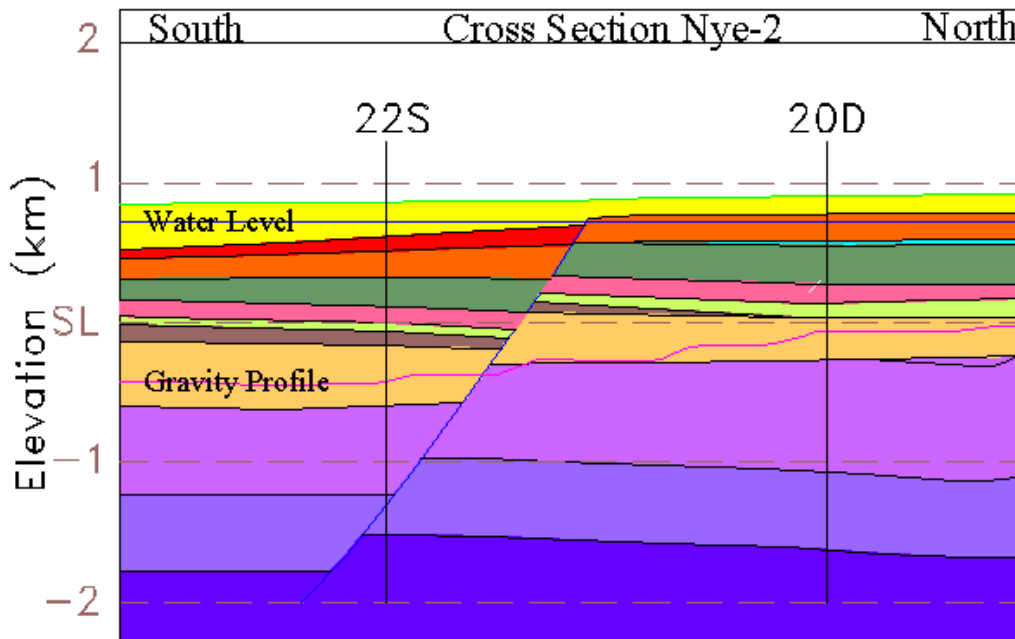
NOTE: Some mapped faults and faults inferred from geophysical anomalies are shown in black. Some Yucca Mountain Site Characterization Project boreholes and Amargosa wells are shown in yellow. Drilled and planned NC-EWDP boreholes are shown in blue.

Figure 1. Location of Cross Sections Nye-1, Nye-2, and Nye-3

These differences provide support for the presence of the buried east-trending faults, such as the Highway 95 fault and other buried fault splays that are part of cross sections Nye-1 and Nye-2. These lithostratigraphic differences also suggest that the Highway 95 fault may play an important role in juxtapositioning rock types of differing hydrologic properties near the southernmost extent of tuff exposures at Yucca Mountain. Selection of an easterly trend for cross section Nye-1 near Highway 95 provided an opportunity to interpolate thicknesses of Paleozoic and Late Proterozoic strata exposed near their eastern and western terminations to the middle of the section near borehole NC-EWDP-2DB. Interpolation of thicknesses, coupled with the consideration of offsets of strata along buried structures, suggests that the pre-Tertiary rocks encountered between depths of 813.8 and 937.3 m (2,670 and 3,075 ft) in NC-EWDP-2DB represent strata of either Silurian or Ordovician age. These strata are a part of the hydrogeologic unit referred to as the lower carbonate aquifer.

Cross section Nye-2 (Figure 2) was constructed, for the most part, along the strike of the Tertiary deposits. On the basis of the nearly horizontal Tertiary strata and the locations of buried faults

that were interpreted from aeromagnetic anomalies (Figure 1), the location where flow paths pass from volcanic rock to alluvium is currently interpreted to occur in the area between NC-EWDP-22S and NC-EWDP-20D, more than 16 km (10 mi) from the potential repository area. The location is important because of the importance of sorption in the alluvium. While there is no matrix diffusion in the alluvium, the sorption capability of the alluvium is more important for some radionuclides, such as neptunium. The amount of sorption in the alluvium is directly proportional to the length of flow path in the alluvium, which depends on the shape and direction of the flow path as well as the location of the transition zone where the water table and flow paths transition from the volcanic tuffs to the alluvium. The uncertainty in the transition zone is been addressed by the Nye County wells as described above, while the flow path direction is addressed in Section 3.4.



NOTES: This figure shows the interpreted location where flow pathways pass from volcanic rock into alluvium (horizontal scale equals the vertical scale). Refer to Figure 1 for relative location of this segment of the cross section Nye-2. Undivided Quaternary and Tertiary alluvium is shown in yellow; younger volcanic rocks and the Timber Mountain Group in red; Paintbrush Group in orange; Wahmonie Formation in cyan; Crater Flat Group in dark green; Tertiary sedimentary rocks below the Tram Tuff in pink; Lithic Ridge Tuff in light green; Tertiary sedimentary strata below the Lithic Ridge Tuff in dark brown; older Tertiary sedimentary rocks in light brown. Blues and purple represent Paleozoic strata. The gravity profile is shown with a pink line.

Figure 2. Generalized Segment of Cross Section Nye-2 in the Vicinity of the Planned Boreholes NC-EWDP-22S and NC-EWDP-20D

Some of the observations discussed above indicate that groundwater flow in the SZ originating from Yucca Mountain includes flow through a portion of the porous alluvium in the area near the southern boundary of the controlled area. Information from borehole NC-EWDP-19D1 is somewhat ambiguous with regard to the groundwater flow path in the alluvium because it has not been established whether greater groundwater flow would be expected in the alluvium or in the underlying volcanic unit. Between NC-EWDP-22S on the south and borehole

NC-EWDP-20D on the north (Figure 2), the flow enters the alluvium—the question of exactly where is based on interpretation discussed in Volume 1 of *FY01 Supplemental Science for Performance Analyses* (BSC 2001a).

The cross sections and associated geologic interpretations will be used as refinements to the hydrogeologic framework for the site-scale SZ flow and transport model as they are developed.

### **3.2 HYDROCHEMISTRY DATA FROM NEW NYE COUNTY EARLY WARNING DRILLING PROGRAM WELLS**

During fiscal year 2001, samples were collected from nine NC-EWDP wells and from USW VH-1 and USW VH-2. These samples were analyzed for major ions, trace elements, stable isotopes, and radiogenic isotopes.

Since July of 2000, 14 sample sets have been collected from the Alluvial Testing Complex (ATC). In addition to identifying changes in water chemistry during long-term pump testing, many of these samples were collected to investigate vertical differences in groundwater within the alluvial aquifer. Although the water chemistries of the various zones at the ATC are similar, several small but consistent variations in isotopic content persist.

### **3.3 HYDRAULIC AND TRACER TESTING AT THE ALLUVIAL TESTING COMPLEX**

The SZ testing program at the ATC has generated a considerable amount of additional data and also conducted several interpretive analyses of these data since publication of the *FY01 Supplemental Science for Performance Analyses* (BSC 2001a). The following paragraphs summarize the additional information that has been obtained through testing efforts.

Single-well injection-withdrawal tracer testing in the alluvium at the NC-EWDP-19D1 location (the location of the ATC), just outside the southwestern corner of the Nevada Test Site, was completed on April 25, 2001. In Volume 1 of *FY01 Supplemental Science for Performance Analyses* (BSC 2001a), it was reported that the preliminary tracer responses in the single-well tests were consistent with a single-porosity conceptual transport model in the alluvium at this location. The tracer responses from the last of the three tests were incomplete at the time the *FY01 Supplemental Science for Performance Analyses* (BSC 2001a) was written. The solute tracer data from all three tests have now been submitted to the Technical Data Management System, and they still clearly support the conclusion that a single-porosity conceptual transport model applies to the alluvium at the NC-EWDP-19D1 location, at least in the uppermost screened interval in NC-EWDP-19D1. The single-well tracer data were subsequently analyzed by both the U.S. Geological Survey (USGS) and the Los Alamos National Laboratory to obtain estimates of specific discharge in the test interval. Although the two organizations used different analysis methodologies, their preliminary estimates of specific discharge were in reasonably good agreement when the same assumptions were made about effective flow porosity in the alluvium. The USGS specific discharge estimate was 1.5 m/yr (4.9 ft/yr), assuming a flow porosity of 0.1, and Los Alamos National Laboratory estimates ranged from 1.3 to 9.4 m/yr (4.3 to 31 ft/yr) for flow porosities ranging from 0.05 to 0.3. These estimates are consistent with the lognormal distribution of specific discharges assumed in the *FY01 Supplemental Science for*

*Performance Analyses* (BSC 2001a)—mean of 2 m/yr (7 ft/yr) and minima and maxima of 0.2 and 20 m/yr (0.7 and 66 ft/yr), respectively (BSC, in preparation [a]).

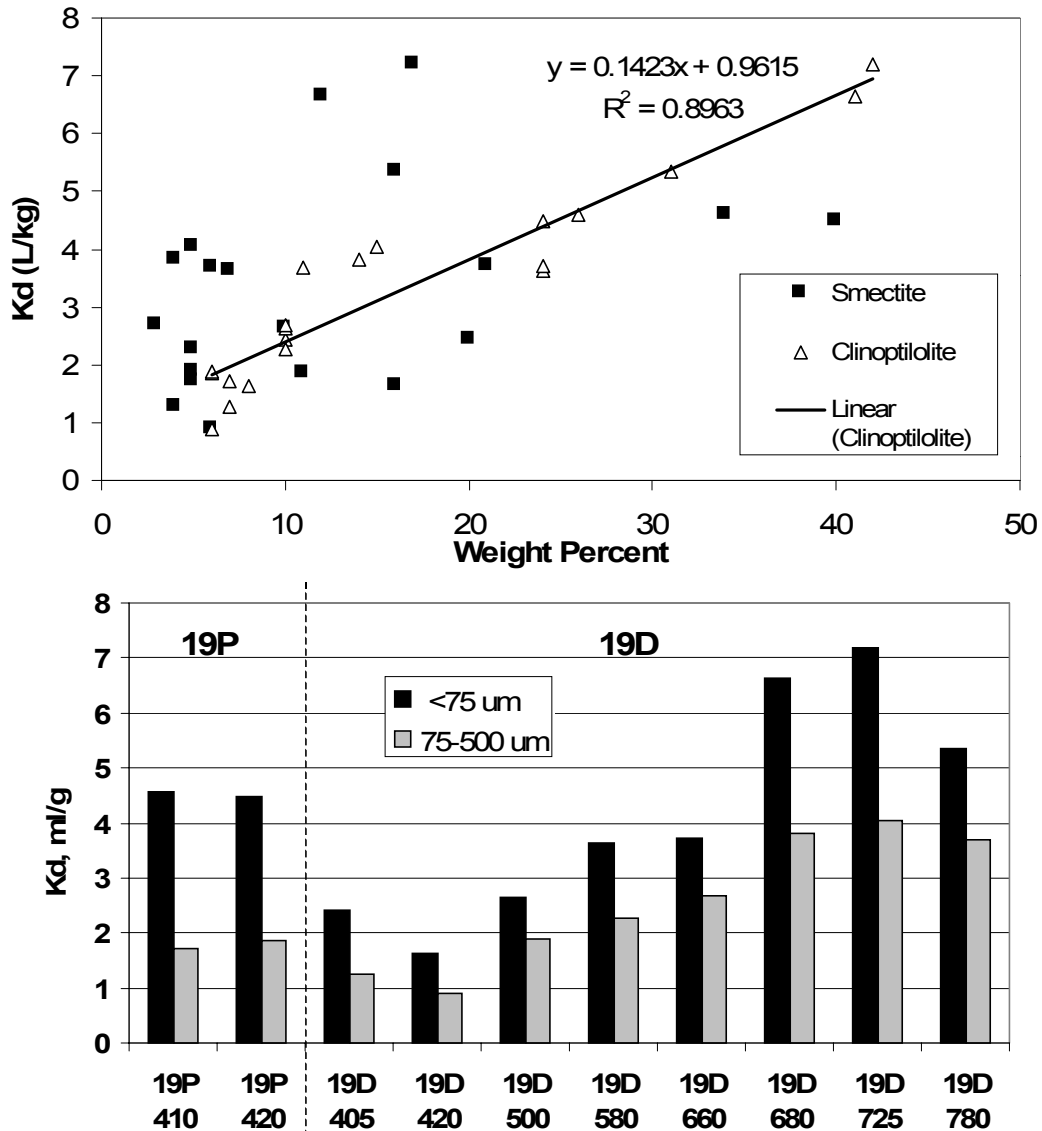
The USGS also completed preliminary analyses of the hydraulic responses during single-well pump testing in NC-EWDP-19D1. The pump tests included one test in which all four screened intervals in the saturated alluvium in NC-EWDP-19D1 were pumped simultaneously and four tests in which each of the four screened intervals in the alluvium were individually pumped after isolating them with packers. The responses in each test were consistent with an unconfined aquifer, and they were therefore analyzed using the unconfined aquifer analytical solution of Neuman (1975). The hydraulic conductivities in the four isolated intervals, assuming that the interval thicknesses were the distance from the water table to the bottom of the sand pack of each interval, were 0.23, 0.02, 0.19, and 0.2 m/day (0.75, 0.04, 0.65, and 0.67 ft/day), for the 1<sup>st</sup>, 2<sup>nd</sup>, 3<sup>rd</sup>, and 4<sup>th</sup> intervals from the surface, respectively. The estimated conductivity of the second interval is considered suspect because there was a clay layer within that interval that likely resulted in an anomalously low transmissivity and conductivity estimates. The combined-interval test yielded a hydraulic conductivity of 0.15 m/day (0.5 ft/day).

Laboratory testing in support of field tracer testing at the ATC has focused on studying the transport behavior of the lithium ion. Both laboratory batch sorption and column transport tests have been conducted in the past year using water and alluvium material from NC-EWDP-19D1 and NC-EWDP-19P (Figure 3). The results have indicated that lithium sorption is highly correlated with the zeolite (clinoptilolite) content of the alluvium, and that sorption generally tends to increase with depth for alluvial materials from the NC-EWDP-19D1 location. Column tests have indicated that lithium may transport faster in the field than batch tests would suggest if lithium concentrations remain relatively high after injection into the aquifer (Figure 4). A three-component cation-exchange model was used successfully to interpret both the batch and column lithium data. This model was also used to make pretest predictions of lithium transport in cross-hole tracer tests at the ATC (to be documented in *Saturated Zone In-Situ Testing* [BSC, in preparation (a)]).

Numerous radionuclide sorption and transport tests not available for inclusion in the supplemental TSPA model have been conducted as part of the SZ testing program in the past year. Recent testing has focused on <sup>129</sup>I, <sup>99</sup>Tc, <sup>233</sup>U, <sup>237</sup>Np, and <sup>239</sup>Pu using water and alluvial material from NC-EWDP-19D1. The former two radionuclides have been tested only in alluvium-packed column experiments. <sup>239</sup>Pu has been tested only in batch sorption experiments. <sup>233</sup>U and <sup>237</sup>Np have been tested in both batch sorption and column transport experiments.

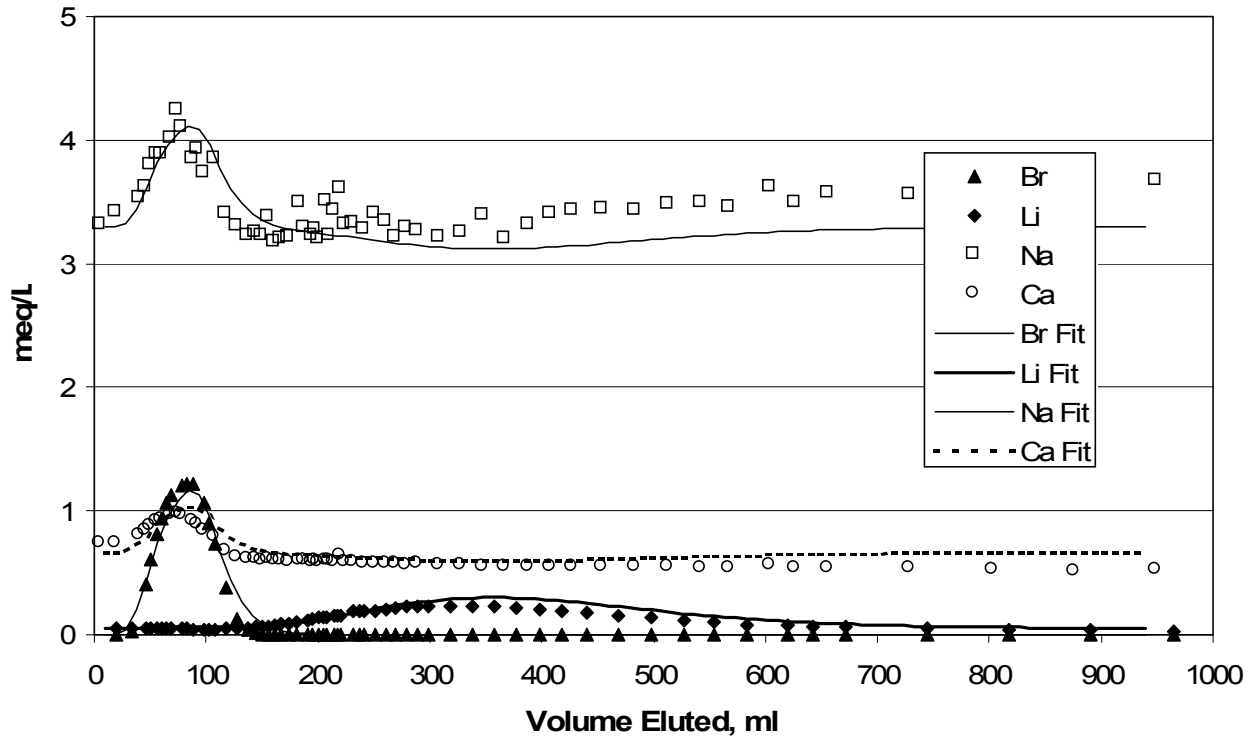
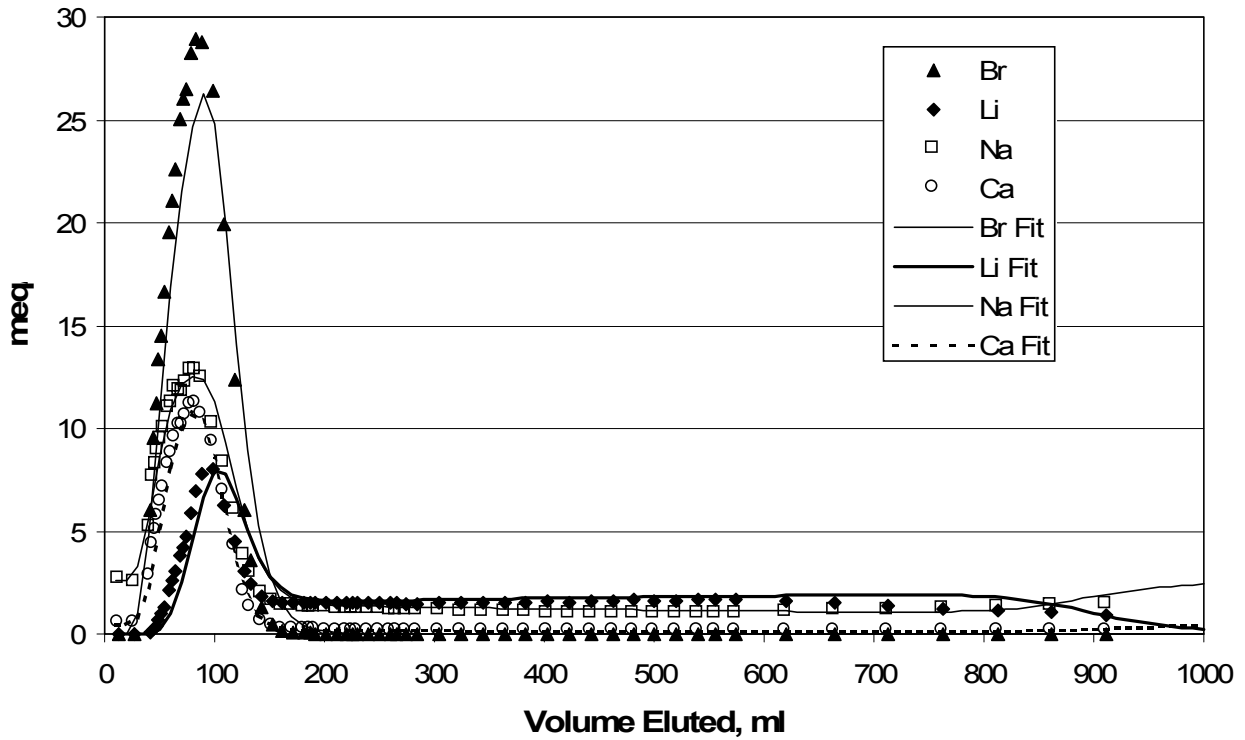
<sup>129</sup>I and <sup>99</sup>Tc showed no apparent retardation in the column experiments under oxidizing (ambient) conditions. <sup>233</sup>U exhibited relatively slow sorption onto alluvium from NC-EWDP-19D1 in batch tests, with  $K_d$  values increasing from 0.9 ml/g after 4 hours of sorption to 3.5 ml/g after 23 days of sorption (although sorption reached an approximate plateau after two days of sorption). <sup>237</sup>Np sorption was stronger than <sup>233</sup>U sorption in batch tests, with  $K_d$  values reaching 3.5 ml/g after 4 hours of sorption and 6.5 ml/g after 20 days of sorption. The stronger sorption of <sup>237</sup>Np relative to <sup>233</sup>U was also observed in column transport tests, where Np was consistently more retarded than U, regardless of the flow rate in the column. Batch desorption experiments confirmed that both <sup>233</sup>U and <sup>237</sup>Np sorption are at least partially reversible with relatively high initial rates of desorption that decrease over time. The column transport behavior

of the Np and U were best modeled as processes in which there was a mass transfer step preceding the sorption onto the alluvium, followed by slow desorption from the alluvium. The preliminary data were not consistent with slow adsorption kinetics. The sorption of  $^{239}\text{Pu}$  onto the alluvium from NC-EWDP-19D1 was very rapid and strong.  $K_d$  values of approximately 1,000 ml/g were measured within six days of sorption, and less than 2 percent of the sorbed Pu desorbed after 30 days of contact with plutonium-free water (BSC, in preparation [a]).



NOTES: The upper panel gives  $K_d$  values for lithium as a function of smectite and clinoptilolite weight percentage in alluvium; the lower panel gives  $K_d$  values for lithium as a function of particle size fraction and interval in wells NC-EWDP-19D and NC-EWDP-19P.

Figure 3. Lithium Distribution Coefficient ( $K_d$ ) Values



NOTE: The LiBr injection concentrations were 0.027 M (top) and 0.0013 M (bottom). There is much less apparent retardation of lithium at the higher injection concentration, but the three-component ion-exchange model can capture this behavior.

Figure 4. Column Data and Model Fits for LiBr Injection Experiments

Finally, experiments intended to compare the transport behavior of carboxylate-modified latex microspheres and silica colloids were conducted in both fractured tuff cores and alluvium-packed columns during the past year. These experiments were conducted to address whether carboxylate-modified latex microspheres can be considered conservative surrogates for inorganic colloids in field tracer tests. Preliminary results have indicated that the carboxylate-modified latex microspheres tested (330-nm diameter) transport conservatively relative to silica colloids (~100-nm diameter) in fractured tuff.

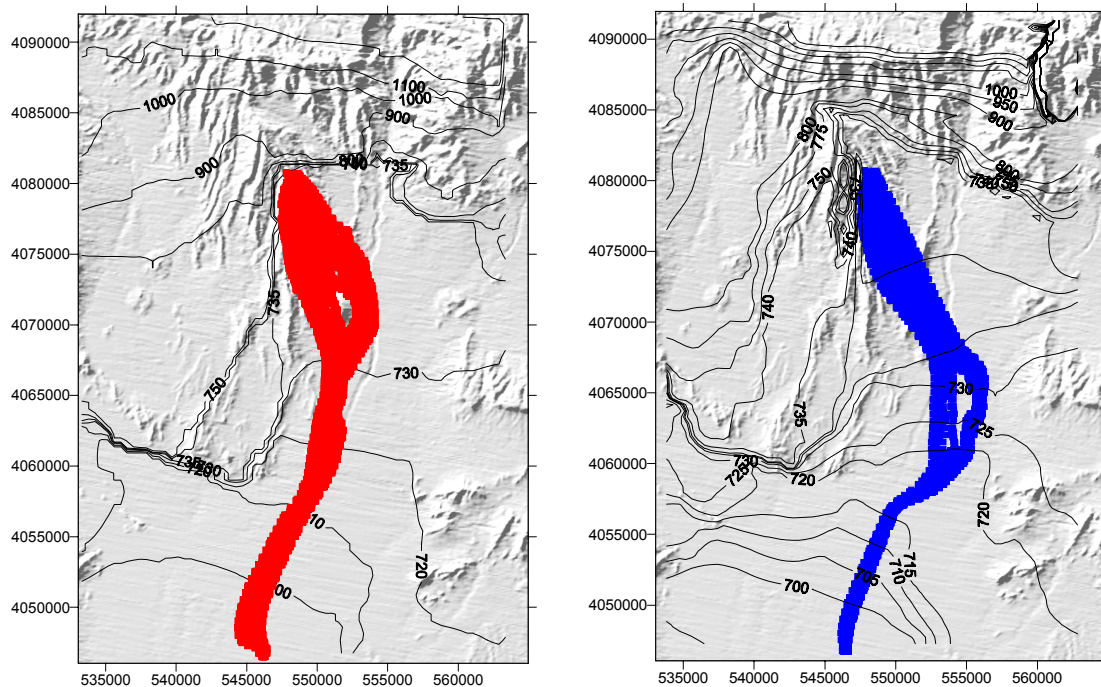
### **3.4 CALIBRATION OF DIFFERENT CONCEPTUAL MODELS OF THE LARGE HYDRAULIC GRADIENT REGION**

The large hydraulic gradient, inferred from hydraulic head measurements made north of the potential repository site at Yucca Mountain, Nevada, has been investigated for many years. Presently, the apparent gradient is simulated in the Yucca Mountain site-scale saturated zone numerical model using a low-permeability east–west feature. Recent work focuses on investigating and calibrating three different conceptual models of the large hydraulic gradient. These models are (1) the current conceptualization described above, (2) a conceptual model that assumes the apparent large hydraulic gradient is due to hydrothermal hydrochemical alteration north of Yucca Mountain, and (3) a conceptual model that includes the observed faults in the northwest–southeast trending washes in northern Yucca Mountain. The combination of the Los Alamos code FEHM (Zyvoloski, Robinson, Dash et al. 1997a; 1997b) and the parameter estimation code (PEST; [Watermark Computing 1994]) was used to calibrate the large three-dimensional computer models. The sensitivity of the estimated groundwater flow paths and specific discharge to each of the conceptual models of the large hydraulic gradient was investigated by recalibrating the numerical model under conditions appropriate to each conceptual model and noting the changes in the groundwater flow regime between models. The investigations indicated that fluid pathlines leaving the potential repository area in the newer alternative conceptualizations were similar to those in the original model. These pathlines are shown in Figure 5. The results of this study show that the large hydraulic gradient can be explained without a low permeability barrier and that fluid transport from the repository area is independent of the conceptualization of the large hydraulic gradient.

#### **3.4.1 Different Conceptualizations of the Solitario Canyon Fault and the Effects on Flow Direction**

The parameterization of the Solitario Canyon fault is an important part of the SZ site–scale flow and transport model because it can potentially control flow from Crater Flat to Fortymile Wash. This flow, in turn, is important in determining the flow paths from the water table beneath the potential repository to the accessible environment and the amount of alluvial material along the flow paths. The original model as well as the two models representing the newer conceptualizations incorporated the Solitario Canyon fault as an anisotropic permeability feature with a calibrated permeability value across the fault (east–west) and 10 and 1,000 times higher values in the north–south and vertical directions, respectively. The fault extended from the bottom of the model to the top of the water table. To investigate the importance of the Solitario Canyon fault to the flow-path direction and specific discharge, two different renditions of the fault were incorporated into the models representing the newer conceptualizations. These were a shallower version that extended from the water table surface to the top of the carbonate aquifer,

and a version that replaced permeability as a calibration parameter with a permeability multiplier. The permeability multiplier version of the fault was considered because the Solitario Canyon fault is a scissors fault with more exposed high-permeability Bullfrog Tuff in the northern part of Yucca Mountain than in the southern part. Thus, it was thought that by using a permeability multiplier instead of an absolute permeability as a calibration parameter, the high permeability window in the north would be retained in at least a relative sense. The calibration using this parameterization again produced very similar results to the original model. Preliminary results of the investigations indicated that the specific discharge and flow direction were not dependent on any particular conceptualization of the Solitario Canyon fault. In the various calibrations, it was a combination of the permeability parameters associated with the Bullfrog Tuff and the Solitario Canyon fault that impacted the flow direction and specific discharge.



NOTES: Pathlines in red on the left indicate flow paths simulated with the original SZ site-scale flow and transport model (BSC 2001b). The blue pathlines on the right indicate flow in the newer conceptualizations (DTN: LA0105GZ12213S.002). The figures also show the predicted water level contours.

Figure 5. Flow Paths of the Original Model and the Newer Conceptualizations Predicted by the Site-Scale Saturated Zone Flow and Transport Model

### 3.4.2 The Effect of Perched Water on the Flow Path and Specific Discharge

Perched water was not explicitly modeled in the SZ site-scale flow and transport model, but all three conceptualizations on the large hydraulic gradient produced water levels in wells UE-25 WT#6 and USW G-2 (suspected to be perched) that were 80 to 90 m (260 to 290 ft) lower than the earlier reported water levels. The predicted water levels are about 930 m (3,050 ft) in this area to the north of Yucca Mountain, which is consistent with the latest USGS water-level interpretation in that area (USGS, in preparation).

### 3.4.3 Vertical Hydraulic Gradient Map

The vertical hydraulic gradient is an important consideration in the specific discharge because of the possibility of vertical gradients to move flow paths between adjacent units, especially where conductive faults exist. In *Calibration of the Site-Scale Saturated Zone Flow Model* (BSC 2001b), Figure 6 shows a map of the vertical gradient in the SZ site-scale model. Shown in plan view are the vertical gradients at the contact between the regional carbonate aquifer and the hydrogeologic unit above it. The results are for the model that was described in this analysis model report. By comparing Figure 6 with Figure 3 in the *Calibration of the Site-Scale Saturated Zone Flow Model* (BSC 2001b), it can be seen that upward vertical gradients exist throughout the flow path region to the south and east of Yucca Mountain. It is also noted that the upward gradient in the model develops primarily from relative head drop in the carbonate aquifer versus the less permeable volcanic confining unit within the site-scale model. The predicted upward gradient in the model probably underestimates the actual upward gradient (one observation at UE-25 p#1 and Nye County well EWDP-2D) because the specified head boundary conditions used on all sides force zero vertical flow at the boundaries. Nevertheless, the pervasive upward gradient along the flow path gives confidence that fluid leaving the repository area remains shallow and in the expected hydrogeologic units.

### 3.4.4 The Effect of Anisotropy on the Specific Discharge

The original SZ site-scale model includes a vertical to horizontal anisotropy ratio of 0.1 in many of the units as described in Section 6.16 of *Calibration of the Site-Scale Saturated Zone Flow Model* (BSC 2001b). The included faults are generally modeled as anisotropic features that are highly conductive in the strike and vertical directions and of low conductivity in the direction across the faults (BSC 2001b, Table 6). The ratios were not varied for the research described in *Calibration of the Site-Scale Saturated Zone Flow Model* (BSC 2001b). The predominate north-south trending faults in the vicinity of Yucca Mountain were represented in an alternate model, also described in *Calibration of the Site-Scale Saturated Zone Flow Model* (BSC 2001b, p. 51) as a north-south to east-west anisotropy ratio in the permeability. The area to which the anisotropy was applied is bounded by a quadrilateral with points (548712, 4065570), (554390, 4067050), (553647, 4080900), (547317, 4081090) in UTM coordinates in plan view and from the top of the water table down to 200 m (660 ft) above sea level in depth. Because the SZ site-scale grid is aligned with these directions, these become principal directions on the permeability tensor. In *Calibration of the Site-Scale Saturated Zone Flow Model* (BSC 2001b), this effect was investigated by rerunning the SZ calibrated model with a 5:1 permeability ratio. This ratio is likely to be changed once the current analysis of the C-wells data is completed. The resulting run was extremely close to the original in all aspects. In fact, the calibration was slightly better. Fluid particle tracking was not performed with the horizontal permeability anisotropy. It is likely that the fluid pathlines leaving the potential repository would have a more north-south trajectory than the original model, thus likely to encounter less alluvium than the original representation of no horizontal permeability anisotropy. The effect of anisotropy in the area described above was also investigated using the models representing the newer conceptualizations of the large hydraulic gradient. Calibration results were similar to those of the original model described in *Calibration of the Site-Scale Saturated Zone Flow Model* (BSC 2001b).

### 3.4.5 Calibration with Modification of Southern Wells

A cluster of Amargosa wells near the southern boundary of the site-scale model domain (between 545000 E and 551000 E) has reported water levels that reflect current conditions rather than predevelopment levels. This will bias the SZ calibration results because these wells are part of the calibration data set. Thus, the southern site-scale specified head boundary condition has also been influenced by recent drawdown and does not reflect predevelopment levels. It was decided that the sensitivity of the SZ calibrated flow model to these two factors should be investigated and a recalibration of the SZ site-scale model carried out. A value of 5 m (16 ft) was added to heads for wells located between 545000 E and 551000 E and extending north in a half-ellipse of radius 4 km (2.5 mi). In addition, 5 m (16 ft) were added to the boundary heads between 545000 E and 551000 E. This is not a precise correction of the well heads and boundary heads but should provide a reasonable estimation of the corrections needed in unit permeabilities and also provide sensitivity of unit permeabilities to the pre- and postdevelopment water levels in that area. The USGS estimated the drawdown in the producing wells near the southern SZ model boundary to be about 5 m (16 ft).

An initial recalibration was carried out using PEST (Watermark Computing 1994). This calibration achieved a reduction in the total PEST-weighted residual of about 50 percent, a significant drop. The permeability parameters of this new calibrated model were close to those of the original model with the important Bullfrog Tuff permeability decreasing slightly and most alluvial and valley-fill permeabilities increasing in value. The southern boundary flux increased about 730 kg/s to about 805 kg/s, which is closer to the flux value from the Death Valley Regional Model (D'Agnese et al. 1997) of about 900 kg/s.

In summary, this study indicated that the southern boundary conditions of the site-scale model are important to the fluid flow in the alluvium region of the model.

### 3.4.6 The Effect of Temperature on Specific Discharge from the Repository Area

Temperature effects are potentially important in the study of fluid pathlines in the site-scale area because of the sensitivity of fluid viscosity to temperature. To understand this sensitivity, two model runs were performed. The model runs used a previously calibrated model of the SZ site-scale (representing the newer conceptualization of the large hydraulic gradient) and raised the fluid temperature in a large area surrounding the repository to 80°C (180°F). Models predict a maximum increased temperature of 65° to 70°C (149° to 158°F) at the water table, compared to the average ambient temperature of 30°C (86°F) (DOE 2001a, Section 4.2.2.3.1). To ensure bounding all potential future temperature effects, 80°C (180°F) was used for this analysis. The area to which the temperature change was applied is bounded by a quadrilateral with points (543000, 4070000), (550000, 4070000), (550000, 4080000), (543000, 4070000) in UTM coordinates in plan view and from the top of the water table down to 200 m (660 ft) above sea level in depth. The fluid pathlines leaving the repository remained in the Bullfrog Tuff. The model transport times change as a result of the lowered viscosity. Thus, if the region outlined above changes from an average of 30°C to 80°C (90°F to 180°F), the transport times decrease in inverse proportion to the change in viscosity. For these temperatures, the transport-time decrease is a factor of two, reflecting the decrease in viscosity. Since the Bullfrog Tuff has at least an

order of magnitude greater permeability than the surrounding units, increase in temperature will affect viscosities and, therefore, transport time, but there is no impact on the flow paths.

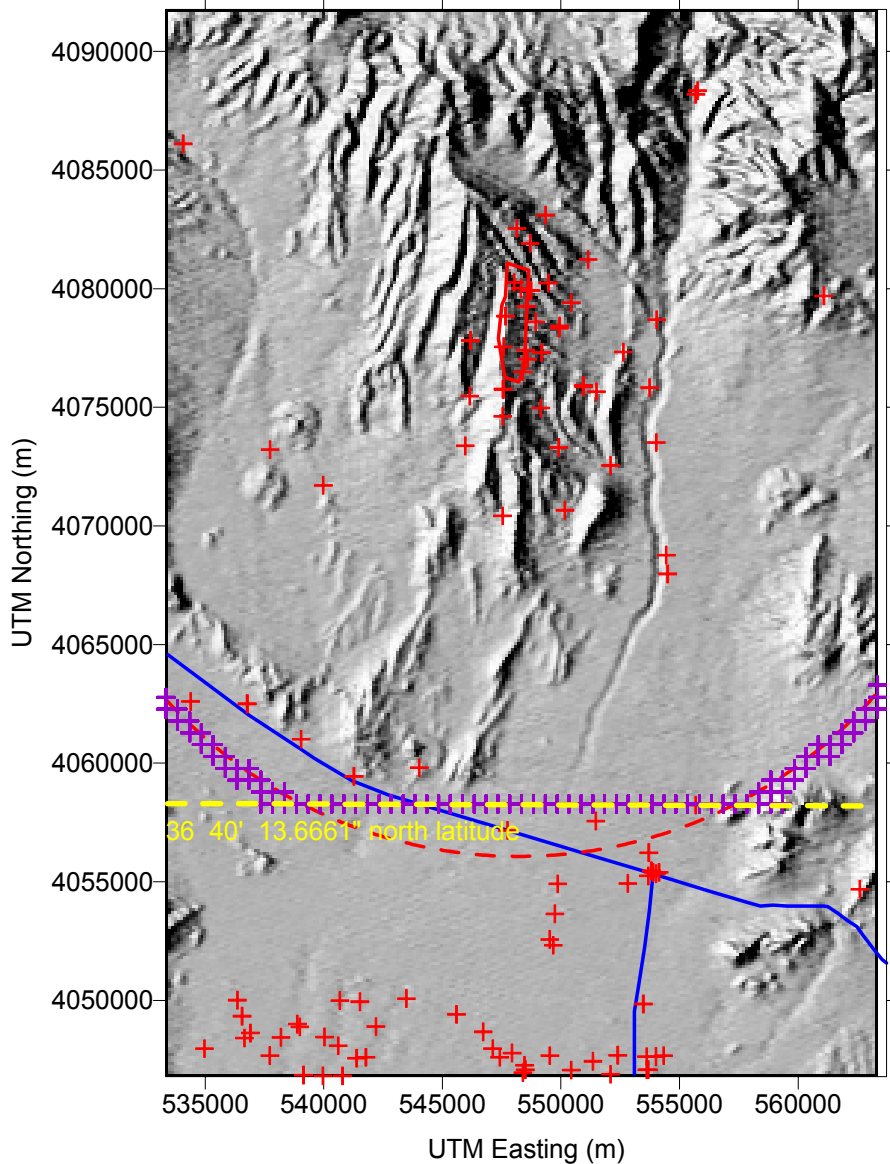
The model run with increased carbonate temperature did not affect directly any pathlines; this is expected because the fluid pathlines remain in the hydrogeologic units above the carbonate aquifer. An increase in the carbonate aquifer temperature increased the effective permeability in that aquifer and actually enhanced slightly the upward hydraulic gradient along the flow path.

### **3.5 EVALUATION OF BOUNDARY TO THE ACCESSIBLE ENVIRONMENT**

This section provides an evaluation of changes in the regulatory definition of the controlled area boundary to the accessible environment with regard to radionuclide transport in the SZ. This evaluation is based on simulation results at the subsystem level (i.e., with the SZ site-scale flow and transport model) and constitutes an expansion of the preliminary analyses presented in Volume 2 of *FY01 Supplemental Science for Performance Analyses* (BSC 2001c) to include all radionuclides considered in the TSPA-SR model. These simulation results were incorporated into the revised supplemental model reported in the *Total System Performance Assessment—Analyses for Disposal of Commercial and DOE Waste Inventories at Yucca Mountain—Input to Final Environmental Impact Statement and Site Suitability Evaluation* (BSC 2001d).

The recently issued U.S. Environmental Protection Agency (EPA) and NRC regulations, 40 CFR 197.12 and 10 CFR 63.302 (66 FR 55732), respectively, specify the controlled area boundary as follows: (1) the surface area, identified by passive institutional controls, that encompasses no more than 300 km<sup>2</sup> (116 mi<sup>2</sup>) and (2) the subsurface underlying the surface area. The surface area must not extend farther south than 36° 40' 13.6661" north latitude, in the predominant direction of groundwater flow, and no farther than 5 km (3 mi) from the repository footprint in any other direction. The evaluation presented in this section is concerned only with the revised definition of the controlled area boundary in the predominant direction of groundwater flow. The boundary to the accessible environment corresponds to the controlled area boundary.

The location designated for the evaluation of regulatory compliance is at the point above the highest concentration of radionuclides in the simulated plume of SZ contamination where the plume crosses the southernmost boundary of the controlled area (at a latitude of 36° 40' 13.6661" North) and reaches the accessible environment. This southern boundary is approximately 18 km (11 mi) from the southern boundary of the potential repository footprint, compared to the original distance of approximately 20 km (12 mi) used in the SZ transport modeling for the TSPA-SR model, as shown in Figure 6. The model nodes along the southern boundary of the controlled area shown in Figure 6 follow the latitude specified by the EPA and NRC regulations in the region where the simulated radionuclide plume crosses the boundary. The model nodes at the boundary near the eastern and western edges of the model domain follow the 20-km (12-mi) arc. Although exhaustive visualization of particle paths for all realizations was not performed, it is expected that all simulated radionuclide paths cross the boundary at the specified latitude. To evaluate compliance with the EPA and NRC regulations, additional SZ breakthrough curves were calculated for all radionuclides used in the TSPA analyses to simulate radionuclide transport from the water table beneath the potential repository to a defined downgradient location using the revised definition of the controlled area boundary.



NOTE: The yellow dashed line represents the southernmost boundary between the controlled area and the accessible environment (36° 40' 13.6661" North latitude as per EPA 40 CFR 197.12 and NRC 10 CFR 63.302 [66 FR 55732]). The red dashed line represents the 20-km fence used in TSPA-SR model to evaluate compliance with proposed EPA and NRC regulations. The purple crosses represent SZ model grid cells at the intersection of the new southernmost boundary with the 20-km fence used in the TSPA-SR evaluations. The red crosses are well locations, and the blue lines represent Highway 95 and Highway 373.

Figure 6. Southernmost Boundary of the Controlled Area and the Accessible Environment

An additional 100 realizations of the SZ site-scale flow and transport model were performed to generate simulated breakthrough curves at the newly defined boundary. These breakthrough curves are strictly SZ breakthrough with time zero as the time when radionuclides hit the water table. Other stochastic parameters for the SZ simulations use the same values that were used in the breakthrough curves for the supplemental TSPA analysis documented in Volume 2 of *FY01 Supplemental Science for Performance Analyses* (BSC 2001c). The simulated radionuclide breakthrough curves at 18 km (11 mi) have somewhat shorter transport times than those at 20 km

(12 mi) as presented in *FY01 Supplemental Science for Performance Analyses* (BSC 2001c) supplemental analysis on a realization-by-realization basis. In particular, those radionuclides that may have significantly greater sorption in the alluvium than in the volcanic units (e.g.,  $^{237}\text{Np}$ ) exhibit significantly shorter transport times to the 18-km (11-mi) boundary relative to the 20-km (12-mi) boundary. This result is related to the fact that the 18-km (11-mi) boundary represents a decrease of travel distance through the alluvium relative to the 20-km (12-mi) boundary.

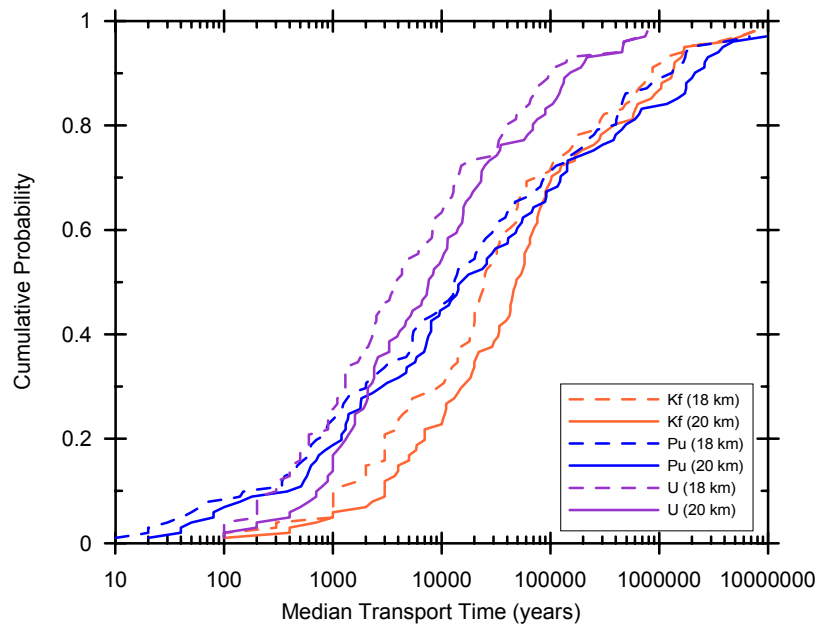
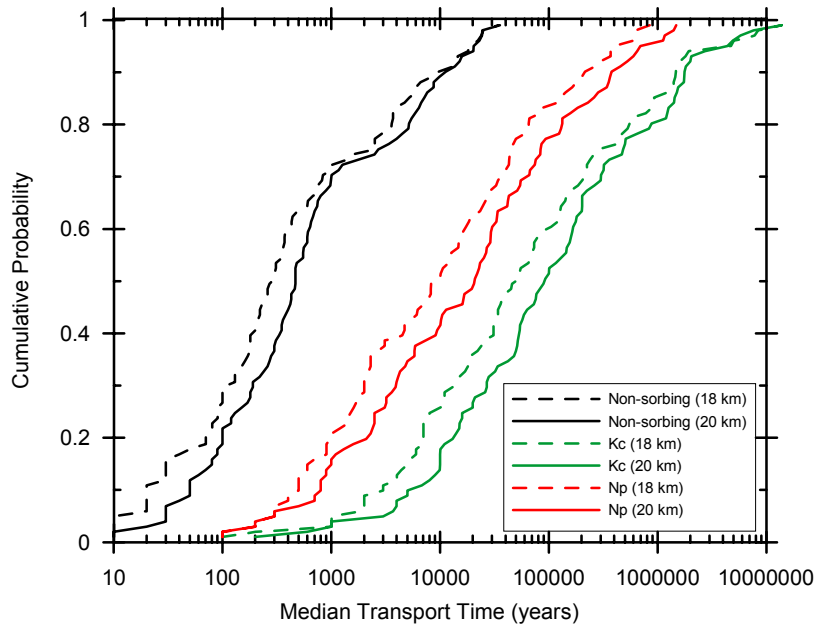
The results of the SZ transport simulations to the newly defined 18-km (11-mi) boundary are summarized and compared to the results to the 20-km (12-mi) boundary in Figure 7. The plots in this figure show the ranked values of the median transport time (e.g., the mid-point of the simulated breakthrough curve) for 100 realizations versus cumulative probability. These plots indicate a reduction in median transport time of up to approximately a factor of two (at a given level of cumulative probability) for transport to the 18-km (11-mi) boundary relative to the 20-km (12-mi) boundary. The average differences in the cumulative distribution functions of median transport time at 18 km (11 mi) and 20 km (12 mi) are somewhat greater for  $^{237}\text{Np}$  and the reversible colloids than for  $^{14}\text{C}$ ,  $^{99}\text{Tc}$ ,  $^{129}\text{I}$ , the irreversible colloids, and uranium.

### **3.6 PARAMETER SENSITIVITY ANALYSIS**

A sensitivity analysis has been performed to evaluate the relative importance of the uncertain parameters included in the three-dimensional SZ site-scale model used for TSPA. This type of analysis provides a method for assessing the results of the SZ site-scale model independently of the TSPA model results. This analysis was performed at the SZ site-scale model level because sensitivity analyses performed at the TSPA level can mask the importance of parameters at the subsystem level. Parameter importance can also be masked if the model uses bounding values and models.

#### **3.6.1 Stepwise Linear Regression Method**

The method used to explore the effects of input parameters on SZ transport in this study was stepwise regression, which is a form of regression analysis. Stepwise regression varies from commonly used multiple regression techniques in that stepwise regression, in addition to calibrating a predictive equation, uses statistical criteria for selecting which of the predictor variables will be included in the final regression equation (McCuen 1985). The stepwise process consists of building the regression equation one variable at a time by adding at each step the variable that explains the largest amount of the remaining unexplained variation (Haan 1994). The coefficient of determination,  $R^2$ , represents the fraction of the total variation that is explained by the linear relationship between the input variables and the dependent variable. The change in the coefficient of determination, as each variable is added into the regression equation, is used to determine the relative importance of each variable. Alpha values were used in part to determine when to stop adding variables to the regression equation. Alpha values can be used as a criterion for assessing variable importance because they provide an indication of how viable the relationships between the independent and dependent variable appears in an analysis (Helton and Davis 1999). A criterion value of 0.01 for alpha was used to determine if a variable was added to the regression.



NOTE: Nonsorbing radionuclides include  $^{14}\text{C}$ ,  $^{99}\text{Tc}$ ,  $^{129}\text{I}$ .  $K_c$  is reversible colloid-facilitated transport of highly sorbing radionuclides;  $K_f$  is reversible colloid-facilitated transport of moderately-high-sorbing radionuclides; and Pu is irreversible colloid-facilitated transport.

Figure 7. Cumulative Distribution Functions of Simulated Median Transport Times for Radionuclides to 18-km and 20-km Distances

Regression analyses can perform poorly when the relationships between the input and output variables are nonlinear (Helton and Davis 1999). Rank transformation of the variables can resolve the problems associated with poor linear fits to nonlinear data (Iman and Conover 1979). Rank transformation was used in this sensitivity analysis to give useful sensitivity results in spite of the nonlinearity between the independent and dependent variables.

### 3.6.2 Regression Analysis Results

The analysis presented here is based on the results of the supplemental TSPA analysis. The dependent variable analyzed for the sensitivity study is the median transport time for each radionuclide at a distance of approximately 18 km (11 mi) from the repository. Figure 8 shows the results of the sensitivity analysis. The figure displays changes in the  $R^2$  values as each variable was added into the stepwise regression model. Variables were no longer added to the regression analysis if the change in  $R^2$  was less than 0.02 and/or the alpha values were greater than 0.01. The results indicate that the median transport time is most sensitive to variation in groundwater specific discharge, with one exception. The retardation factor in the alluvium for irreversible colloids (CORAL) was more important than the groundwater specific discharge parameter for the simulations of irreversible colloid transport. A possible explanation is that the CORAL parameter has considerable uncertainty and spans many orders of magnitude.

#### Legend

GWS = Groundwater specific discharge  
 CORAL = Retardation factor for irreversible colloids in the alluvium  
 FPVO = Flowing interval porosity  
 DCVO = Effective diffusion coefficient  
 FISV = Flowing interval spacing  
 FPN = Northern boundary of the alluvium  
 KD9 = Reversible colloid sorption coefficients for actinides (Am, Pu, Pa, Th) matrix/alluvium for the Kc model  
 KD10 = Reversible colloid sorption coefficients for fission products (Cs and Sr) matrix/alluvium for the Kc model  
 KDNP = Sorption coefficient for Np the alluvium  
 KDUA = Sorption coefficient for U in the alluvium

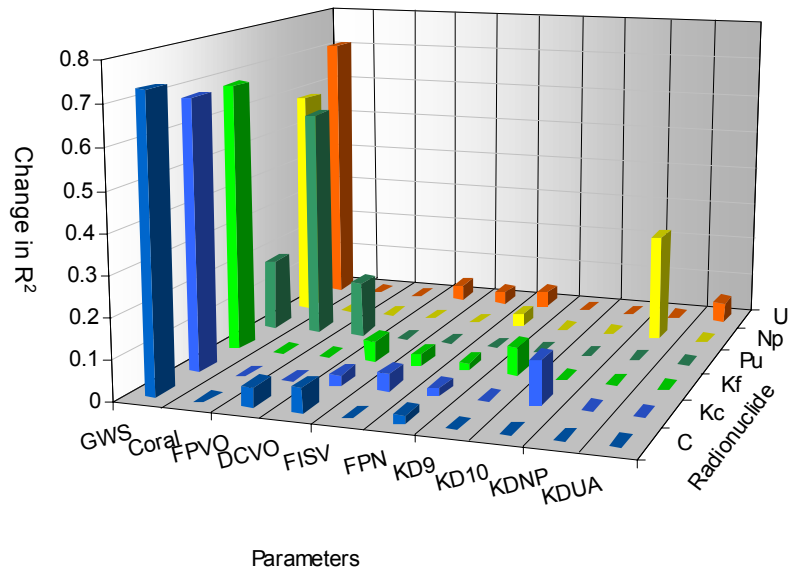


Figure 8. Coefficient of Determination ( $R^2$ ) Change per Step in the Stepwise Regression Analysis for each Radionuclide

The second most important parameters for sorbing radionuclide simulations were sorption coefficient parameters. The sorption coefficient for Np in the alluvium is the second most important variable for the Np simulations. The second most important parameter for the U simulations was the sorption coefficient in the alluvium for uranium (KDUAL). The next most important parameters for the U simulations were the effective diffusion coefficient (DCVO), the flowing interval spacing (FISV), and the extent of the northern boundary of the alluvium (FPN). For the case of nonsorbing carbon transport, the most important parameters after groundwater specific discharge are parameters related to matrix diffusion. The parameter DCVO and the flowing interval porosity (FPVO) are the second and third most important parameters, respectively. The sensitivity results for the reversible colloidal transport simulations

( $K_f$  and  $K_c$ ) are similar to the uranium simulations as shown in Figure 8 with the second most important parameter for their simulations being the respective sorption coefficients in the matrix and alluvium (KD9 and KD10) for  $K_f$  and  $K_c$ .

It should be noted that the sensitivity analysis done at the TSPA-SR level found that for very long time periods (100,000 years), groundwater specific discharge is the fourth most important parameter in determining simulated dose among all of the parameters that are input to the TSPA-SR simulations (CRWMS M&O 2000a). The waste package parameters dominate in importance for earlier time periods.

### **3.7 URANIUM MILL TAILINGS SITES AS ANALOGUES FOR TRANSPORT OF RADIONUCLIDES IN ALLUVIUM AT YUCCA MOUNTAIN**

The evaluation of uranium mill tailings sites as potential analogues for the transport of radionuclides in alluvium at Yucca Mountain has continued. The work has focused on the two Uranium Mill Tailings Remedial Action (UMTRA) Project sites that show the most promise in terms of providing information of use to Yucca Mountain site evaluations. These two sites are located in Gunnison and Rifle, Colorado, respectively. The reason only 2 out of the 24 potential UMTRA sites were chosen for more detailed evaluation is that a large amount of information is required for each site in order to derive useful information regarding transport behavior. Most of the UMTRA sites do not have sufficiently detailed information available to allow these sorts of evaluations.

The Gunnison UMTRA site (DOE, in preparation) is located on a drainage divide between the Gunnison River and Tomichi Creek. It is underlain by approximately 33.5 m (110 ft) of floodplain alluvium. The average depth to groundwater is approximately 1.5 m (5 ft). Although the tailings pile was removed from the site between 1992 and 1995, tailings seepage has contaminated the unconfined alluvial aquifer beneath and downgradient from the site. Because sulfuric acid was used extensively in the processing of ores at the site, tailings seepage was enriched in sulfate. Sulfate is a conservative (nonsorbing) constituent in these alluvial groundwater systems and can be used to trace the maximum extent of travel of contaminants from the site. A sulfate plume has been delineated in the alluvial aquifer that extends up to 2,000 m (7,000 ft) downgradient from the site. In plan view, the shape of the plume is quite narrow, suggesting only limited lateral dispersion of sulfate as it was transported downgradient. The concentrations of sulfate are similar in much of the plume suggesting both dispersion and dilution effects were very limited in this hydrologic setting. To the extent that the hydrologic properties of alluvium at Yucca Mountain are similar to those of the alluvium at the Gunnison site, the evaluation of this site suggests the processes of dispersion and dilution of radionuclides may have limited impact on the transport of radionuclides over distances of several kilometers in the alluvial portion of the Yucca Mountain flow system. Additional data obtained through the ATC and Nye County on the hydrology of alluvium downgradient of Yucca Mountain will be required to fully evaluate the potential impact of the Gunnison site observations.

The New Rifle UMTRA site (DOE 1999) is located adjacent to the Colorado River in western Colorado. The site is underlain by 6 to 9 m (20 to 30 ft) of alluvium deposited by the Colorado River. Underlying the alluvium are sandstones and shales of the Tertiary Wasatch Formation. The depth to groundwater beneath the site is 2 to 3 m (5 to 10 ft). Removal of the tailings pile at

this site was completed in 1996. As at the Gunnison site, seepage from the tailings pile at the New Rifle site was enriched in sulfate. This sulfate has been transported in alluvial groundwater to a maximum distance of approximately 5,790 m (19,000 ft) downgradient from the site. As with the Gunnison site, evidence for lateral dispersion is limited at the New Rifle site. In this case, however, the geometry of the downgradient alluvial deposits naturally limit lateral dispersion. Dilution does appear to be an important process at this site based on the hydrochemical evaluation. Waters from the underlying Wasatch Formation appear to be the primary diluent.

The transport of uranium at the New Rifle site is of particular interest to the Yucca Mountain Project because uranium is a major component of nuclear waste to be emplaced in a repository. Analyses of uranium in alluvial groundwater suggest that uranium has been transported almost as far as sulfate in this flow system. A retardation factor of 1.4 was calculated for uranium based on its maximum travel distance relative to sulfate. This value for the retardation factor corresponds to an average sorption coefficient of 0.06 mL/g. Batch sorption coefficients obtained in laboratory experiments with samples of alluvium from the site and an artificial groundwater show a range of -0.3 to 1.4 mL/g with an average value of 1.0 mL/g. An analysis of potential causes for the difference between the field-derived value for the uranium sorption coefficient (0.06 mL/g) and the laboratory value (1.0 mL/g) suggests relatively minor variations in water chemistry can have major impacts on the sorption behavior of uranium in these transport systems. In the case of New Rifle, the fact that an artificial water was used in the laboratory experiments may be significant. In laboratory sorption experiments for the Yucca Mountain site, natural ground waters from the site are used. This minimizes the potential impact of variations in water chemistry on the measured sorption coefficients.

### **3.8 A REALISTIC CASE OF SATURATED ZONE FLOW AND TRANSPORT**

The saturated zone flow and transport model is the culmination of much data collection, analysis, conceptual model development, numerical model calibration, and model validation. It covers the entire saturated flow and transport from the water table below the potential repository to the accessible environment. Consequently, there is substantial uncertainty about portions of the model, particularly in the transition zone where the water table transitions from being in the volcanic tuffs to being in the alluvium. In addition due to the complexity of the physical system and processes, simplifications are necessary for modeling flow and transport throughout the model domain. Following standard engineering practice, these uncertainties and simplifications have been treated conservatively so that confidence in the model results is as high as possible.

As part of an overall emphasis on the best characterization possible of uncertainties, an effort to develop a Realistic Case model was started. This effort will be documented in the *Saturated Zone Flow Patterns and Analysis* (BSC, in preparation [b]), a series of studies are being conducted to evaluate the impact of conservatism used as a result of conservatism and simplification.

#### **3.8.1 Preliminary Saturated-Zone Realistic-Case Model**

The preliminary realistic-case model for SZ flow and transport uses a reasonable set of parameter values for the assessment of groundwater flow and transport from beneath the potential

repository footprint to the accessible environment at a distance of approximately 18 km (11 mi) (Figure 6). The SZ realistic-case model constitutes a reassessment of the SZ flow and transport system that supplements the stochastic model used for the TSPA-SR analyses. The SZ realistic-case model differs from the expected-value TSPA-SR simulation of SZ flow and transport (CRWMS M&O 2000b) in several ways.

- The higher value of effective diffusion coefficient ( $2.0 \times 10^{-10} \text{ m}^2/\text{s}$ ) in fractured tuff units that is appropriate for water
- A higher value of flowing interval porosity (0.01) in fractured tuffs
- The more northerly location of the tuff/alluvium contact for the alluvial uncertainty zone
- Groundwater flow field with lower permeability (by a factor of 2) in the alluvial uncertainty zone
- The location of the accessible environment at approximately 18 km (11 mi) south of the repository footprint (versus 20 km [12 mi] for the TSPA-SR simulations).

The resulting groundwater breakthrough curve using these combined realistic-case parameter values in the SZ site-scale flow and transport model is shown in Figure 9. Travel times in the leading portion of the realistic-case model breakthrough curve have been increased primarily by the lower permeability in the alluvial uncertainty zone and by the higher fracture porosity. Travel times in the trailing portion of the realistic-case model breakthrough curve have been increased more by the higher effective diffusion coefficient and the more northerly boundary of the alluvial uncertainty zone. The simulated travel times for the entire breakthrough curve are shorter for the approximately 18-km (11-mi) distance to the accessible environment than for the 20-km (12-mi) boundary used in the TSPA-SR model (CRWMS M&O 2000a).

### **3.8.2 Cumulative Unsaturated Zone/Saturated Zone Realistic-Case Breakthrough Curve**

The results of the UZ flow and transport modeling realistic case are used as input for assessing the cumulative travel time in the UZ and SZ, from the potential repository to the accessible environment at the 18-km (11-mi) distance. The long dashed line in Figure 9 shows the breakthrough curve for tritium from the potential repository to the water table from the UZ site-scale model. The UZ breakthrough curve is for present-day climate and the expected perched water/CHn fracture model. Also shown in Figure 9 is the breakthrough curve for the preliminary SZ realistic-case model. Note that this SZ breakthrough curve in Figure 9 was simulated using a “smeared” source at the water table beneath the potential repository, as opposed to the point source used in the sensitivity analyses. The potential-repository-wide source at the water table is more appropriate for combining with the UZ transport simulation results.

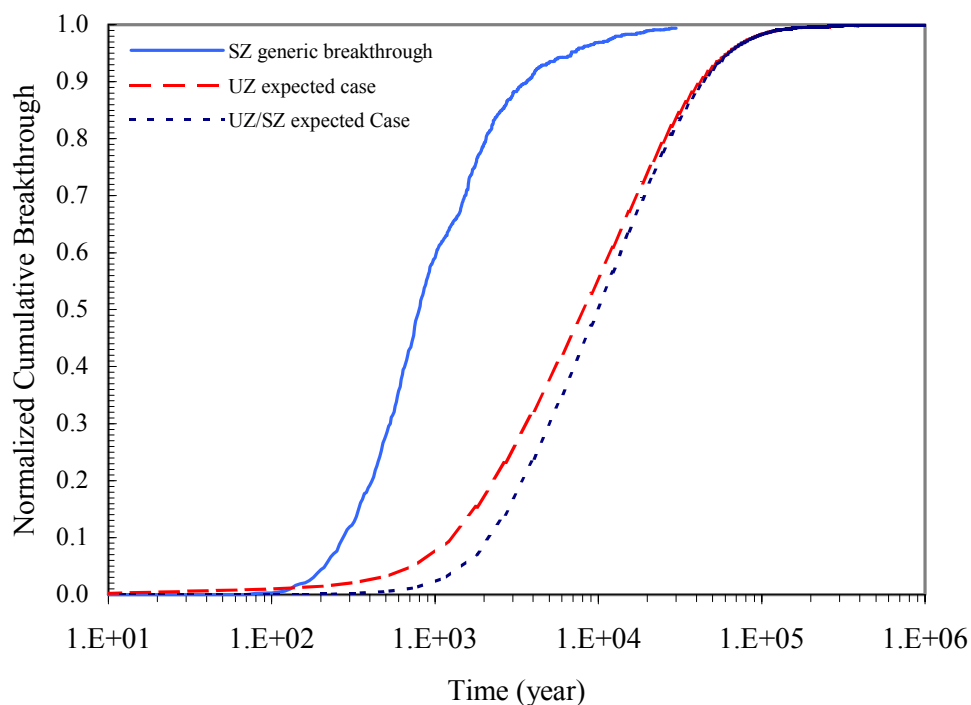


Figure 9. SZ Realistic Case Normalized Cumulative Breakthrough Curve based on Unsaturated Zone Realistic Case Input at Water Table.

To simulate transport efficiently in the SZ, the convolution approach (Zyvoloski, Robinson, Birdsell et al. 1997) is used to calculate the radionuclide breakthrough curve at the accessible environment. The SZ realistic breakthrough curve for the nonsorbing tracer at the accessible environment is shown in Figure 9 as the solid blue line. This curve shows a first arrival time of about 100 years and a 50 percent arrival time of about 800 years. It takes about 3,640 years for 90 percent of the injected nonsorbing tracer to travel from the water table under the repository to the accessible environment. Using the realistic breakthrough curve as the response function and the UZ realistic-case breakthrough at the water table as the input, the UZ/SZ realistic-case breakthrough curve (Figure 9) at the accessible environment was calculated with the convolution approach (Zyvoloski, Robinson, Birdsell et al. 1997).

### 3.8.3 Examination of Saturated Zone Realistic-Case Breakthrough Curves in the Context of Carbon-Isotope Data from Borehole NC-EWDP-2D

The use of groundwater carbon-14 data from a well located approximately 18 km (11 mi) downgradient from the repository along an estimated flow path offers one potential means of assessing the reliability of the combined UZ/SZ travel-time estimates. In this assessment, groundwater data from well NC-EWDP-2D is used (CRWMS M&O 2000a, Table 3). This well is about 20 km (12 mi) downgradient from the potential repository along the groundwater flow path (CRWMS M&O 2000b, Figure 7). If the combined UZ/SZ travel times are accurate, then the mean travel time from the calculated distribution should approximate the groundwater carbon-14 age at this well once allowances have been made to account for differences in the flow

path lengths of the water particles associated with each analysis. The carbon-14 age of groundwater represents the time of travel of water from the ground-surface to the sampling well, whereas the combined UZ/SZ groundwater travel time distribution represents the time of travel from the repository horizon to a hypothetical well located 18 km (11 km) from the repository horizon. Because most of the combined UZ/SZ travel time is estimated to result from the transport of water through the unsaturated zone, the differences unsaturated zone path lengths (approximately 500 m [1,600 ft]) are likely to be more important to groundwater age than differences in saturated-zone path lengths. Therefore, an important step in comparing the UZ/SZ groundwater travel times and groundwater carbon-14 age is to calculate the travel times from the ground surface to the repository and remove this time from the groundwater carbon-14 age before it is compared to the calculated UZ/SZ travel-time distribution.

The travel time from the ground surface to the potential repository horizon can be estimated by assuming that rapid fracture flow through the welded units results in negligibly small travel times through these units and that most of the travel time from between the ground surface and potential repository horizon is the result of slow matrix flow through the nonwelded tuffs of the PTn. The travel time through the PTn is calculated from the average moisture content of rocks in the PTn (20 percent) and the PTn thickness. The PTn ranges in thickness from about 100 m (330 ft) in the northern end of the repository to 25 m (80 ft) in the southern end of the repository area. Complete piston displacement of the in situ water will be assumed in order to maximize the estimated travel time through the PTn and thereby highlight the possible importance of adjusting the groundwater age for travel time through the upper unsaturated zone. Assuming piston displacement, the water column heights of 20 m (66 ft) (for a 100-m (330-ft) thick PTn) and 5 m (16 ft) (for a 25-m [80-ft] thick PTn) are divided by the average flux over the repository (5 mm/yr or 0.005 m/yr [0.2 in.]), resulting in a travel time through the PTn of 4,000 to 1,000 years. Therefore, groundwater carbon-14 ages should be 1,000 to 4,000 years older than the mean UZ/SZ travel time if other aspects of the deeper unsaturated zone and saturated zone are being modeled accurately.

The median combined UZ/SZ travel time is about 10,000 years (Figure 9). For the measured carbon-14 activity ( $^{14}\text{A}$ ) of 25 percent modern carbon (pmc) of groundwater at NC-EWDP-2D, the age of the groundwater depends on the initial  $^{14}\text{A}$  of the groundwater ( $^{14}\text{A}_0$ ). The value of  $^{14}\text{A}_0$  can be less than long-term atmospheric concentrations of roughly 100 pmc because of the effects of geochemical processes both in the unsaturated zone and in the saturated zone. Table 1 shows the ages of groundwater with a measured  $^{14}\text{A}$  of 25 pmc calculated for different assumed values of  $^{14}\text{A}_0$  and the radioactive decay law:

$$t = (-1/\lambda) \ln (^{14}\text{A}/^{14}\text{A}_0) \quad (\text{Eq. 1})$$

where

- t is the mean groundwater age (years)
- $\lambda$  is the radioactive decay constant ( $1.21 \times 10^{-4}$  years<sup>-1</sup>)
- ln is the natural logarithm.

Table 1. Calculated Groundwater Ages for Different Assumed Values of  $^{14}\text{A}_0$  and Measured  $^{14}\text{A}$  of 25 pmc

$^{14}\text{A}_0$	Actual mean groundwater age (years)
100	11,457
95	11,033
90	10,586
85	10,114
80	9,613
75	9,079
70	8,509
65	7,897
60	7,235
55	6,516
50	5,728

The distribution of the combined UZ/SZ travel times shown in Figure 9 can also be used to estimate the equivalent  $^{14}\text{A}$  of a water having these travel times. This equivalent  $^{14}\text{A}$  can then be compared to the measured groundwater  $^{14}\text{A}$  at well NC-EWDP-2D. This comparison implies that, like that calculated travel-time distribution, the groundwater at well NC-EWDP-2D may also be a mixture of groundwater that has traveled along different flowpaths or along the same flowpath at different velocities. The equivalent groundwater  $^{14}\text{A}$  activity associated with the travel-time distribution ( $\overline{^{14}\text{A}}$ ) can be calculated directly from the travel-time distribution by calculating the  $^{14}\text{A}$  of each parcel of water based on its travel time and weighting this value of  $^{14}\text{A}$  by the fractional volume of water ( $\Delta V_w$ ) associated with this travel time:

$$\overline{^{14}\text{A}} = \sum_{i=1}^n \Delta V_w \text{ } ^{14}\text{A} \quad (\text{Eq. 2})$$

where  $^{14}\text{A}$  is calculated from the radioactive decay law:

$$^{14}\text{A} = ^{14}\text{A}_0 e^{-\lambda t} \quad (\text{Eq. 3})$$

It is evident from these equations that the value of  $\overline{^{14}\text{A}}$  associated with the travel-time distribution depends on the assumed value of  $^{14}\text{A}_0$ . The values of  $\overline{^{14}\text{A}}$  associated with the travel-time distribution are given for different values of  $^{14}\text{A}_0$  in Table 2. The calculations indicate that travel-time distribution has an  $^{14}\text{A}$  of 25 pmc or greater if  $^{14}\text{A}_0$  exceeds about 80 pmc.

Table 2. Equivalent Carbon-14 Activity ( $\overline{{}^{14}A}$ ) Calculated from the Combined UZ/SZ Travel-Time Distribution for Different Assumed Values of  ${}^{14}A_0$

${}^{14}A_0$	$\overline{{}^{14}A}$
100	31.1
90	28.0
80	24.9
70	21.8
60	18.6
50	15.5

The preceding analysis has highlighted the need to obtain a reliable estimate of  ${}^{14}A_0$ . A variety of methods have been used to estimate the value of  ${}^{14}A_0$  to use with the radioactive decay law (Clark and Fritz 1997, Chapter 8). To correct for the effects of calcite dissolution, a process that would tend to decrease  ${}^{14}A_0$ , a simple method was used that compares the total dissolved inorganic carbon (DIC) in the recharge water ( $m_{DIC-R}$ ) with the DIC of the downgradient groundwater ( $m_{DIC-GW}$ ):

$$q_{DIC} = \frac{m_{DIC-R}}{m_{DIC-GW}} \quad (\text{Eq. 4})$$

where  ${}^{14}A_0 = q_{DIC} \times 100 \text{ pmc}$ . This method assumes that once infiltration has reached the saturated zone and become recharge, the water is effectively isolated from further interaction with carbon dioxide gas ( $\text{CO}_2$ ) in the unsaturated zone, so that any downgradient increases in the DIC of the groundwater are a result of interactions with carbon-bearing minerals. These minerals are assumed to be depleted in carbon-14, which is probably the case because most saturated zone calcite was formed either during a 10 million-year-old hydrothermal event or to deposition under unsaturated conditions at a time when the water table was lower than today (Whelan et al. 1998). Thus, although the proportions of dissolved  $\text{CO}_2$ , bicarbonate ( $\text{HCO}_3^-$ ), and carbonate ( $\text{CO}_3^{2-}$ ) may change with pH as the groundwater interacts with the rock, the total DIC is fixed unless the groundwater reacts with calcite. The method also assumes that the recharge water itself requires no corrections for calcite dissolution, a topic that will be discussed further below.

In this analysis, the chemical characteristics of recharge water are assumed to be the same as the deep perched water from boreholes SD-7 and UZ-14 (CRWMS M&O 2000a, Table 7). The  ${}^{14}A$  of deep perched water probably does not require corrections to account for interactions with calcite at shallower depths. This assessment is based on the good agreement between in the relationship between  ${}^{36}\text{Cl}/\text{Cl}$  ratios and  ${}^{14}A$  values of the perched water and relationships established between the isotopes from pack-rat midden studies (CRWMS M&O 2000a, Section 6.5.4.2.2). It is further supported by studies of pedogenic calcites in the Great Basin that indicate that isotopic exchange between soil gas and percolating water in the unsaturated zone will re-establish the isotopic characteristics of the water to reflect those of the soil gas after the water has interacted with shallow calcite (Quade and Cerling 1989; Quade et al. 1990).

Based on the pH and  $\text{HCO}_3^-$  concentrations of the perched water samples pumped from these boreholes, perched water has a DIC concentration between 128.3 mg/L (SD-7) and 144 mg/L  $\text{HCO}_3^-$  (UZ-14). Based on its pH and  $\text{HCO}_3^-$  concentrations, the DIC concentration of groundwater at well NC-EWDP-2D is 149 mg/L  $\text{HCO}_3^-$  (CRWMS M&O 2000a, Table 3). Using these values with the preceding expression for  $q_{\text{DIC}}$ , one obtains an estimate for  $q_{\text{DIC}}$  of between 0.86 and 0.97. The corresponding estimates for the  $^{14}\text{A}_0$  of the groundwater at well NC-EWDP-2D are 86 and 97 pmc.

For the  $^{14}\text{A}_0$  values of 86 and 97 pmc estimated from the downgradient increases in DIC concentrations, the measured  $^{14}\text{A}$  value of 25 pmc at well NC-EWDP-2D results in a carbon-14 age of 10,200 to 11,200 years. To remove the effects of travel time from the ground surface to the potential repository horizon from the groundwater carbon-14 age so that this age is more directly comparable to the calculated combined UZ/SZ travel-time distribution, the carbon-14 ages must be decreased by 1,000 to 4,000 years. This results in adjusted groundwater ages that range from 6,200 to 10,200 years. The lower adjusted carbon-14 age of 6,200 years indicates that the combined UZ/SZ travel times are too slow and that actual transport is faster than has been modeled. The upper adjusted groundwater carbon-14 age of 10,200 years is nearly identical to the mean calculated UZ/SZ travel time.

### **3.9 SATURATED ZONE RESULTS FROM THE ATOMIC ENERGY OF CANADA LIMITED BUSTED BUTTE EXPERIMENTS.**

Interesting additional data have been obtained from the unsaturated and the saturated block transport studies. In these studies, the transport rates of selected radionuclides are studied in blocks excavated from Busted Butte. Basically, water containing radionuclides is injected into one end of a block and collected from the opposite end. Measured transport rates of radionuclides of interest relative to a conservative constituent such as tritium can be used to calculate retardation coefficients. These retardation coefficients can be used to derive sorption coefficients which can, in turn, be compared with sorption coefficients derived from batch or column tests using crushed rock material. These comparisons provide tests of the suitability of the use of batch sorption coefficients in the prediction of transport in solid rock.

The most recent results obtained on the unsaturated block transport experiment indicate that the conservative tracer (a dye) has not yet broken through to the sampling ports at the base of the block. In the saturated block experiment, the tracer has broken through at several of the sampling ports. In this experiment, transport is expected to occur along approximately horizontal flow lines between the input port and the extraction port. The flow regime has been found to be more complicated than expected with flow focused upward along the injection borehole wall then along the upper surface of the block and finally down along the extraction borehole wall. The recent installation of a peristaltic pump appears to have corrected this short-circuiting of the intended flow regime. The recent data also indicate that the Eh of the water extracted from the block is quite reducing. The pore water in Busted Butte from where the block was obtained is most likely oxidizing. A reducing condition could enhance the retardation of radioelements such as neptunium and technetium in the block test relative to the retardation that would occur under natural conditions in Yucca Mountain. The retardation behaviors of the elements cobalt, cesium, and sodium have been evaluated from data obtained through dissection

of the trial block experiment. The retardation observed for these elements is consistent with the results of batch experiments using crushed rock material.

#### **4. IMPLICATIONS OF RECENT TEST RESULTS AND OTHER ADDITIONAL INFORMATION**

##### **4.1 STRATIGRAPHY OF THE NYE COUNTY EARLY WARNING DRILLING PROGRAM BOREHOLES**

The lithologic data continue (1) to enhance our understanding of the flow and transport in the SZ from beneath the potential repository horizon to the accessible environment and (2) to reduce the uncertainty in the location of the transition zone where the water table transitions from being in the volcanic tuffs to being in the alluvium. That location is currently interpreted to occur in the area between NC-EWDP-22S and NC-EWDP-20D. In the meantime, uncertainty about the length of the flowpath through the alluvium is included in numerical simulations (CRWMS M&O 2000b, Section 6) of the site-scale SZ flow and transport for the TSPA-SR model (CRWMS M&O 2000a).

##### **4.2 HYDROCHEMISTRY DATA FROM NEW NYE COUNTY EARLY WARNING DRILLING PROGRAM WELLS**

The hydrochemistry data continue to indicate that groundwater recharge occurs at higher elevations north of Yucca Mountain through Fortymile Wash and through Yucca Mountain itself. Flow away from Yucca Mountain is generally southeast toward Fortymile Wash, then south to the Amargosa Valley. The issues of flow stratification, mixing with water from Fortymile Wash, the existence of more southerly flow paths, and the location of the transition from fracture flow to porous medium flow in the alluvium remain subject to a large range of uncertainty until the next phase of the Nye County Drilling Program is completed to help reduce the uncertainty. The additional data do not disagree with the general discussion of flow and transport presented in the YMS&ER (DOE 2001a).

##### **4.3 HYDRAULIC AND TRACER TESTING AT THE ALLUVIAL TESTING COMPLEX**

Data from the ATC continue to confirm the conceptual model of flow and transport in the alluvium and provide information on flow and transport to reduce uncertainty in the modeling parameters.

##### **4.4 CALIBRATION OF DIFFERENT CONCEPTUAL MODELS OF THE LARGE HYDRAULIC GRADIENT REGION**

Sensitivity analyses completed using the site-scale SZ flow and transport model to investigate the impact of different conceptualizations, representation of hydrogeologic features and the existence of anisotropy yielded similar flow paths. The differences in the flow paths are insufficient to affect the SZ flow fields.

#### **4.5 EVALUATION OF BOUNDARY TO THE ACCESSIBLE ENVIRONMENT**

SZ breakthrough curves generated using the site-scale flow and transport model at the 18-km (11-mi) boundary indicate shorter travel time than at the 20-km (12-mi) boundary. The 18-km (11-mi) boundary results in a flow path in the SZ that reduces the flow path from the potential repository by 2 km (1.2 mi) of alluvium flow path. This will impact the breakthrough curves of all radionuclides to different extents. However, radionuclides subject to sorption in the alluvium, such as neptunium, will see the most impact. These breakthrough curves were incorporated into *Total System Performance Assessment—Analyses for Disposal of Commercial and DOE Waste Inventories at Yucca Mountain—Input to Final Environmental Impact Statement and Site Suitability Evaluation* (BSC 2001d).

#### **4.6 PARAMETER SENSITIVITY ANALYSIS**

A sensitivity analysis at the subsystem level has been performed to evaluate the relative importance of the uncertain parameters included in the three-dimensional SZ site-scale model based on results from the supplemental TSPA model. The results indicate that the median transport time is most sensitive to variation in groundwater specific discharge with one exception. The retardation factor in the alluvium for irreversible colloids was more important than the groundwater-specific-discharge parameter for the simulations of irreversible colloid transport.

#### **4.7 URANIUM MILL TAILINGS SITES AS ANALOGUES FOR TRANSPORT OF RADIONUCLIDES IN ALLUVIUM AT YUCCA MOUNTAIN**

At the New Rifle site, the difference between the field-derived value for the uranium sorption coefficient and laboratory value suggests the coefficient is quite sensitive to differences in the water chemistry used in the laboratory experiments as compared to ground water chemistry at this site. Because natural ground water is used in laboratory experiments to obtain sorption coefficients for the Yucca Mountain flow system, a similar difference between laboratory and field-scale sorption coefficients is not expected. This conclusion will be tested with laboratory and field sorption data for the element lithium. A comparison of dispersion and dilution of contaminants in ground water flow systems associated with the Gunnison and New Rifle UMTRA sites suggests these parameters may be very sensitive to site-specific hydrogeologic conditions over distances of several kilometers. Over longer transport distances, this sensitivity to local conditions is likely much less significant.

#### **4.8 A REALISTIC CASE OF SATURATED ZONE FLOW AND TRANSPORT**

Results of the saturated flow pattern analyses completed using input from the UZ flow pattern analysis indicate a median breakthrough curve (50 percent arrival) of more than 8,000 years. The average breakthrough is longer. The analyses show that no significant arrival occurs in the 1,000-year time frame. The analyses confirm the conservatism used in the models used for TSPA and can be used to identify ways to reduce conservatism in future modeling.

#### 4.9 IMPLICATION OF THE ATOMIC ENERGY OF CANADA LIMITED BLOCK EXPERIMENT

The implications of the results obtained to date are that the transport behavior of Na, Cs and Co, are reasonably well determined in batch sorption experiments. Therefore, batch-derived coefficients for these elements can be used in transport calculations. For Np and Tc, the situation is less clear. If the Eh values measured in the waters extracted from the saturated block test are representative of natural values in the saturated zone and Yucca Mountain, then Np and to a lesser extent Tc would be retarded in the Calico Hills Formation. On the other hand, if the measured Eh values reflect experimental artifacts (e.g., transient microbial activity), the implications of the test results for transport of these elements in Yucca Mountain would be unclear.

#### 5. REFERENCES

66 FR 55732. Disposal of High-Level Radioactive Wastes in a Proposed Geologic Repository at Yucca Mountain, NV. Final Rule 10 CFR Part 63. Readily available.

40 CFR Part 197. Protection of Environment: Public Health and Environmental Radiation Protection Standards for Yucca Mountain, Nevada. Readily available.

AP-2.14Q, REV 2, ICN 0. *Review of Technical Products and Data*. Washington, D.C.: U.S. Department of Energy, Office of Civilian Radioactive Waste Management. ACC: MOL.20010801.0316.

AP-SIII.1Q, Rev. 0, ICN 1. *Scientific Notebooks*. Washington, D.C.: U.S. Department of Energy, Office of Civilian Radioactive Waste Management. ACC: MOL.20000516.0002.

BSC (Bechtel SAIC Company) 2001a. *FY01 Supplemental Science and Performance Analyses, Volume 1: Scientific Bases and Analyses*. TDR-MGR-MD-000007 REV 00 ICN 01. Las Vegas, Nevada: Bechtel SAIC Company. ACC: MOL.20010801.0404; MOL.20010712.0062; MOL.20010815.0001.

BSC 2001b. *Calibration of the Site-Scale Saturated Zone Flow Model*. MDL-NBS-HS-000011 REV 00 ICN 01. Las Vegas, Nevada: Bechtel SAIC Company. ACC: MOL.20010713.0049.

BSC 2001c. *FY01 Supplemental Science and Performance Analyses, Volume 2: Performance Analyses*. TDR-MGR-PA-000001 REV00. Las Vegas, Nevada: Bechtel SAIC Company. ACC: MOL.20010724.0110.

BSC 2001d. *Total System Performance Assessment—Analyses for Disposal of Commercial and DOE Waste Inventories at Yucca Mountain—Input to Final Environmental Impact Statement and Site Suitability Evaluation*. Deliverable ID: SL986M3. Las Vegas, Nevada: Bechtel SAIC Company.

BSC (in preparation [a]). *Saturated Zone In-Situ Testing*. ANL-NBS-HS-000040 REV 00. Las Vegas, Nevada: Bechtel SAIC Company.

BSC (in preparation [b]). *Saturated Zone Flow Patterns and Analyses*. ANL-NBS-HS-000038 REV 00.

Clark, I.D. and Fritz, P. 1997. *Environmental Isotopes in Hydrogeology*. Boca Raton, Florida: Lewis Publishers. TIC: 233503.

CRWMS M&O (Civilian Radioactive Waste Management System Management and Operating Contractor) 2000a. *Total System Performance Assessment for the Site Recommendation*, TDR-WIS-PA-000001 REV 00 ICN 01. Las Vegas, Nevada: CRWMS M&O. ACC: MOL.20001220.0045.

CRWMS M&O 2000b. *Input and Results of the Base Case Saturated Zone Flow and Transport Model for TSPA*. ANL-NBS-HS-000030 REV 00. Las Vegas, Nevada: CRWMS M&O. ACC: MOL.20000526.0330.

D'Agnesse, F.A.; Faunt, C.C.; Turner, A.K.; and Hill, M.C. 1997. *Hydrogeologic Evaluation and Numerical Simulation of the Death Valley Regional Ground-Water Flow System, Nevada and California*. Water-Resources Investigations Report 96-4300. Denver, Colorado: U.S. Geological Survey. ACC: MOL.19980306.0253.

DOE (U.S. Department of Energy) 1999. *Final Site Observational Work Plan for the UMTRA Project New Rifle Site*. GJO-99-112-TAR, Rev. 1. Grand Junction, Colorado: U.S. Department of Energy, Grand Junction Office. TIC: 249902.

DOE 2001a. *Yucca Mountain Science and Engineering Report*. DOE/RW-0539. Washington, D.C.: U.S. Department of Energy, Office of Civilian Radioactive Waste Management. ACC: MOL.20010524.0272.

DOE 2001b. *Yucca Mountain Preliminary Site Suitability Evaluation*. DOE/RW-0540. Washington, D.C.: U.S. Department of Energy, Office of Civilian Radioactive Waste Management. ACC: MOL.20011101.0082.

DOE (in preparation). *Final Site Observational Work Plan for the UMTRA Project Gunnison Site*. Grand Junction, Colorado: Prepared by the U.S. Department of Energy, Grand Junction Office.

EDCON 2000. *Report for the Borehole Gravity Survey in the NC-EWDP-19D Well in Nye County, Nevada on Behalf of TRW Corp*. EDCON Job# 00011. Denver, Colorado: EDCON, Inc. TIC: 249823.

USGS (in preparation). *Water-Level Data Analysis for the Saturated Zone Site-Scale Flow and Transport Model*, ANL-NBS-HS-000034 REV 01.

GS000808314211.005. Interpretations of the Lithostratigraphy in Boreholes NC-EWDP-01DX, NC-EWDP-02D, NC-EWDP-03D, and NC-EWDP-09SX, Nye County Early Warning Drilling Program Phase I, FY 99. Submittal date: 08/14/2000.

Haan, C. 1994. *Statistical Methods in Hydrology*. 1<sup>st</sup> Edition. Ames, Iowa: Iowa State University Press. TIC: 208928.

Helton, J. and Davis, F.J. 1999. *Sampling-Based Methods for Uncertainty and Sensitivity Analysis*. SAND99-2240. Albuquerque, New Mexico: Sandia National Laboratories.

Iman, R.L. and Conover, W.J. 1979. "Use of the Rank Transformation in Regression." *Technometrics*, 21, (4), 499-509. Alexandria, Virginia: American Statistical Association.

LA0105GZ12213S.002. SZ Flow Model With No East-West Barrier. Submittal date: 05/11/2001.

McCuen, R.H. 1985. *Statistical Methods for Engineers*. Upper Saddle River, New Jersey: Prentice-Hall, Inc.

MO0004NC99WL2D.000. Water Level Measurements in Borehole, NC-EWDP-2D, Nye County Early Warning Drilling Program. Submittal date: 04/18/2000.

MO0007NYE02565.024. Cuttings Sample Log for Borehole NC-EWDP-19D. Submittal date: 07/11/2000.

Neuman, S.P. 1975. "Analysis of Pumping Test Data from Anisotropic Unconfined Aquifers Considering Delayed Gravity Response." *Water Resources Research*, 11, (2), 329-342. Washington, D.C.: American Geophysical Union. TIC: 222414.

Quade, J. and Cerling, T.E. 1990 "Stable Isotopic Evidence for a Pedogenic Origin of Carbonates in Trench 14 near Yucca Mountain, Nevada." *Science*, 250, 1549-1552. Washington, D.C.: American Association for the Advancement of Science. TIC: 222617.

Quade, J.; Cerling, T.E.; and Bowman, J.R. 1989. "Systematic Variations in Carbon and Oxygen Isotopic Composition of Pedogenic Carbonate Along Elevation Transects in the Southern Great Basin, United States." *Geologic Society of America Bulletin*, 101, 464-475. Boulder, Colorado: Geologic Society of America. TIC: 224797.

Watermark Computing. 1994. *PEST, Model-independent Parameter Estimation*. Oxley, Australia: Watermark Computing. TIC: 240719.

Zyvoloski, G.A.; Robinson, B.A.; Birdsell, K.H.; Gable, C.W.; Czarnecki, J.; Bower, K.M.; and Faunt, C. 1997. *Saturated Zone Radionuclide Transport Model*. Milestone SP25CM3A. Los Alamos, New Mexico: Los Alamos National Laboratory. ACC: MOL.19980127.0089.

Zyvoloski, G.A.; Robinson, B.A.; Dash, Z.V.; and Trease, L.L. 1997a. *User's Manual for the FEHM Application—A Finite-Element Heat- and Mass-Transfer Code*. Los Alamos National Laboratory Report LA-13306-M. Los Alamos, New Mexico: Los Alamos National Laboratory. TIC: 235999.

Zyvoloski, G.A.; Robinson, B.A.; Dash, Z.V.; and Trease, L.L. 1997b. *Summary of the Models and Methods for the FEHM Application—A Finite-Element Heat- and Mass-Transfer Code*. LA-13307-MS. Los Alamos, New Mexico: Los Alamos National Laboratory. TIC: 235587.